ID-1058

LOW-VELOCITY IMPACT DAMAGE OF KNITTED CARBON FABRIC/EPOXY COMPOSITES

Gao Yang, Chwee Teck Lim and Seeram Ramakrishna
Department of Mechanical Engineering
National University of Singapore, 9 Engineering Drive 1, Singapore 117576

SMMARY: This paper examines low-velocity impact on knitted carbon fabric reinforced epoxy composite and focuses on the impact resistance and damage modes arising from differences in number of plies and lay-ups. Results show that the impact damage patterns are totally different from the usual circular, quasi-squarish or peanut-shaped damage patterns. C-scan images reveal that the impact damage modes are in the form of crossed bands and photographs and stereomicroscopic images demonstrate that the damages also comes in the form of crossed cracks. The major modes of damage and energy absorption are matrix cracking, matrix/fibre debonding and fibre breakage. This composite also has good energy absorption capability with energy absorption ratio reaching about 80%.

KEYWORDS: knitted composites, low velocity impact, IFWI test, damage modes, energy absorption

INTRODUCTION

For the last two decades, conventional composites have been widely used with outstanding success [1-7]. However, high manufacturing costs, poor shapeability, complicated repairing techniques and inferior out-of-plane mechanical properties limit the applications of the first generation composites as primary load-bearing structures. One of the main concerns regarding conventional composites is whether they are able to withstand and contain impact damage without compromising their structural integrity. As a result, efforts have been made to obtain composites with desirable impact resistance and damage tolerance.

Then came textile composites which could incorporate automated manufacturing methods of the textile industry. Highly automated manufacturing techniques of textile industry can improve production and quality of composites at a lower cost. Knitted composite is one such textile composites. Knitted fabrics are characterised by their interlocking loops of yarns. They can be classified under two main types, the warp knit fabrics and the weft knit fabrics according to knitting direction. Due to their low fibre volume fraction and loose loops configuration of fibres, knitted fabric composites usually have poor in-plane mechanical properties than conventional composites as well as woven and braided textile composites [8].

While much research work has been done to explore the mechanical performance as well as use of knitted fabric composites [2, 6, 8-33], not much work has been done to investigate their impact performance [34].

Low-velocity impacts are usually defined as impacts occurring at velocity of not more than 10 m/s [35-38]. At such low impact energy, while non-visible damage may occur, this can significantly reduce the strength of composites. Low-velocity drop impact test is one approach to study the impact performance of composites. The instrumented falling weight impact (IFWI) test is one such method to study the low-velocity impact of composites [35,36]. This paper presents a study on the low-velocity impact of a knitted carbon fabric reinforced epoxy composite. The study aims to determine damage mechanisms, damage modes, impact resistance, impact responses and energy absorption capability of this composite.

EXPERIMENTAL SET-UP

The materials used to fabricate the composite panels are carbon fibre and epoxy. The carbon fibre is Toray T300B yarn, which is used to make the plain weft knitted fabrics. The epoxy contains a resin R-50 and a hardener H-64, mixed in the ratio of 100/48 by weight. A hand lay-up process is exploited for making knitted carbon fabric/epoxy composite panels.

Specimens are cut from the composite panels and consist of 1-ply, 2-ply and 4-ply with different lay-ups. 2-ply specimens include lay-ups of [0/0] and [0/90] while 4-ply specimens include lay-ups of $[0/0]_s$, $[0/45]_s$ and $[0/90]_s$. Here, the wale direction is denoted as 0^o while the course direction as 90^o.

Low-velocity impact tests are conducted using an instrumented falling weight impact (IFWI) test system. The test system comprises four components: a drop tower with a guide column, a set of fixture consisting of two rings with inner diameter of 120mm and outer diameter of 200mm, an impactor and a digital oscilloscope. The impactor is a mild steel cylinder with a hemispherical tip of diameter 42mm. Specimens are clamped using the fixture with an exposed circular area of diameter 120mm. Both the drop height and mass of impactor can be varied to obtain different incident impact energy levels so as to obtained various damages from barely visible impact damage (BVID) to through-thickness damage. Figure 1 shows a schematic diagram of the IFWI test system.

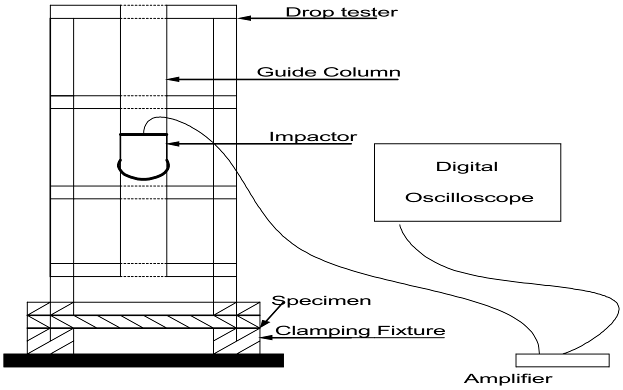

Figure 1 Schematics of IFWI test system

After the impact test, the specimens are inspected for any damage by noting the damage area and damage modes. The damage are observed by visual inspection as well as employing stereomicroscopy and C-scan techniques.

RESULTS AND DISCUSSION

For BVID situations, no visual damage is observed. The stereomicroscopic images show that there are crystalloid damage and some disordered microcracks around the impact spot. In some specimens, slight matrix/fibre debonding is found. Figure 2 describes the damage patterns of $[0/45]_s$ and $[0/90]_s$ specimens when subjected to different incident impact energies (IE). Figure 3 shows representative photographs of damage on the surfaces of specimens. Figure 4 shows the representative stereomicroscopic pictures of matrix/fibre debonding, whitening crystalloid matrix damage and fibre breakage. Here, whitening crystalloid damage is defined as the local whitening of the matrix around the impact spot due to impactor hitting on the matrix.

$[0/45]_s$ specimens	IE	$[0/90]_s$ specimens
No visible damage found	**1.801J**	Microcracks on distal side
Microcracks on distal side	**2.411J**	Whitening crystalloid on matrix on impacted side Cracks on distal side
Whitening crystalloid on matrix on impacted surface Cracks on distal side	**3.013J**	Whitening crystalloid on matrix on impacted surface Cracks growing on distal side
Propagation of cracks on distal surface	**3.618J**	Microcracks on impacted surface Initiation of debonding and Propagation of cracks on distal side
Severe whitening crystalloid on matrix on impacted side Initiation of debonding	**4.278J**	Initiation of cracks on impacted side More debonding on distal side
Microcracking on impacted side More debonding on distal side	**6.035J**	Propagation of cracks on front side Severe debonding
Slight through-thickness cracks	**8.007J**	Crossed whitening crystalloid bands on impacted side Slight through-thickness cracks

Figure 2 Relating impact damage with IE for the 4-ply specimens

With further increase in incident impact energy, visual cracks and through-thickness cracks start to occur. Figure 5 shows representative C-scan images for the $[0/0]_s$ specimen with through-thickness cracks. Here crossed debonding bands along the cracks are clear. Figure 6 shows typical C-scan images for the $[0/45]_s$ specimens with slight cracks on distal surface. Due to smaller IE, the images of cracks are not obvious and no clear debonding bands along the cracks are observed. From the images obtained, the damages are crossed matrix cracks and/or matrix/fibre debonding and the damages possess the following features:

- Matrix cracks cross at nearly right angle in both the wale and the course directions for unidirectional and orthogonally stacked specimens (Fig.3 (a)), while matrix cracks radiate haphazardly for $[0/45]_s$ specimens (Fing.3 (b)). For severe through-thickness crack or crush damage, damage modes may not appear as a single cross shape but may appear as different patterns of cross-cracks (Fig.3 (c)).

- Generally, the crack in the wale direction is longer than that in the course direction. For $[0/45]_s$ specimens, several short cracks cross a longer crack in a haphazard manner. This is evident as the tensile strength in the wale direction is smaller than that of in course direction [21].

(a) [0/90] specimen (IE=4.278J)

(b) $[0/45]_s$ specimen (IE=6.035)

(c) [0/0] through-thickness (IE=4.344)

Figure 3 Photographs of crossed-crack damage on impacted surface

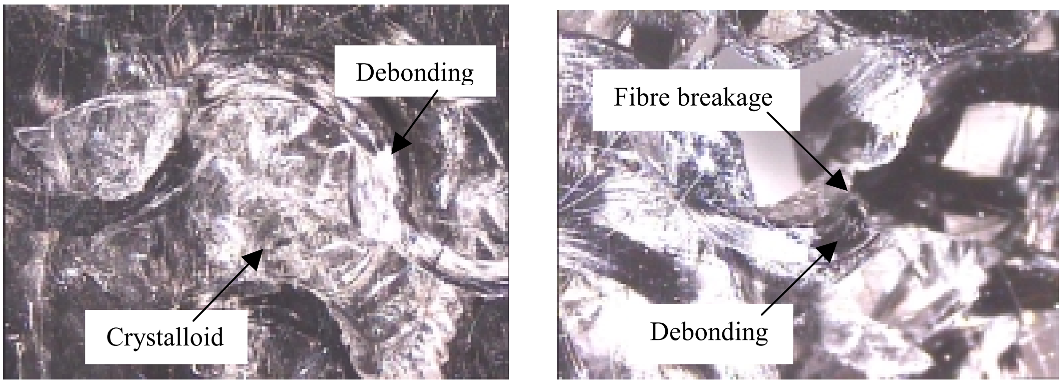

(a) Crystalloid damage and debonding ($[0/0]_s$ specimen, IE=13.629)

(b) Debonding and fibre breakage ([0/0] specimen, IE=3.013J)

Figure 4 Representative stereomicroscopic images of various impact damages

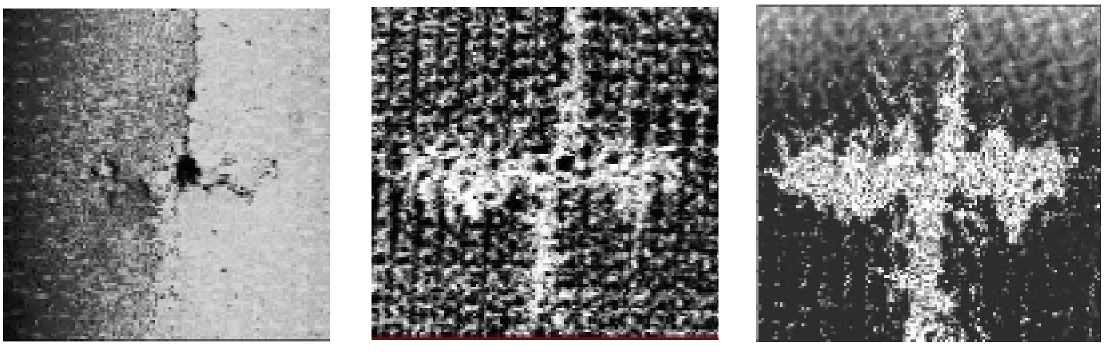

(a) Close to top surface

(b) Mid-depth

(c) Close to distal surface

Figure 5 Typical C-scan images at different depth of a impacted $[0/0]_s$ specimen (IE=10.185J)

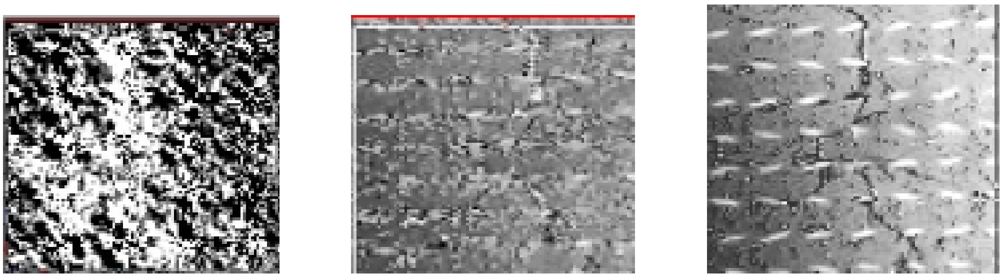

(a) Close to top surface (a) Mid-depth (c) close to distal surface

Figure 6 Typical C-scan images of $[0/45]_s$ specimens (IE=3.013J)

- The cracks on the top-surface (impacted side) are less apparent than that on distal side. It is observed that the impact damage initiates on the distal surface and is more severe than that on the top-surface due to bending of the thin specimens. However, for BVID cases (without visible microcracks), only squeezed crystalloid damage can be found on the top-surface, no damage is observed on the distal side, and C-scan and stereomicroscopic images did not detect any damage.
- No indentation can be observed at the impacted area on the top-surface, even though through-thickness damage has occurred.
- The C-scan images obtained from the mid-depth are of similar shapes with those images obtained from top and distal surfaces.
- The images obtained from C-scan are similar with that obtained from digital camera photographs for all obtainable cases, but for severe cracks like through-thickness cracks, the C-scan images of damage appear in the form of bands rather than cracks. This phenomenon indicates that there is fibre/matrix debonding along cracks.
- No delamination is observed for all incident impact energy levels.
- Different number of plies and lay-ups do affect damage resistance. For instance, $[0/45]_s$ specimens possess greater impact resistance than that of $[0/0]_s$ and $[0/90]_s$ specimens.

Figure 7 shows representative plots of impact force vs. time. It was observed that there exists a threshold value of impact force. When impact force is lower than the threshold value, the force keeps rising and no damage which may lead to reduce stiffness of specimens occurs. But as impact force exceeds the threshold value, the force will initially drop (see IE=6.04J in Fig. 7) or form a force plateau (see IE=3.62J in Fig. 7). This sudden change of impact force slope shows that matrix cracking, and/or matrix/fibre debonding, and/or fibre breakage may have occurred at that moment. Thereafter, impact force continues to reach a maximum before decreasing to zero. There are two situations in which no force drops or force plateaus occur. One is when incident impact energy is too small to make any significant damage. In this situation, no obvious damage can be observed. Another situation is when incident impact energy is great enough so that matrix cracking, matrix/fibre debonding and fibre breakage happen at about the same time and results in loss of load-bearing ability (see IE=12.57J in Fig. 7). Severe through-thickness cracks occur and specimens fail structurally.

Figure 8 to 13 show plots of energy absorption ratio (namely AE-ratio) vs. IE for various stacking sequences with incident impact energy. Generally, for BVID situations, the energy absorption ratio is small. However, energy absorption ratio can be more than 80% when through-thickness damage occurs. Specimens with more layers can bear greater impact force than that with fewer layers, however, the later

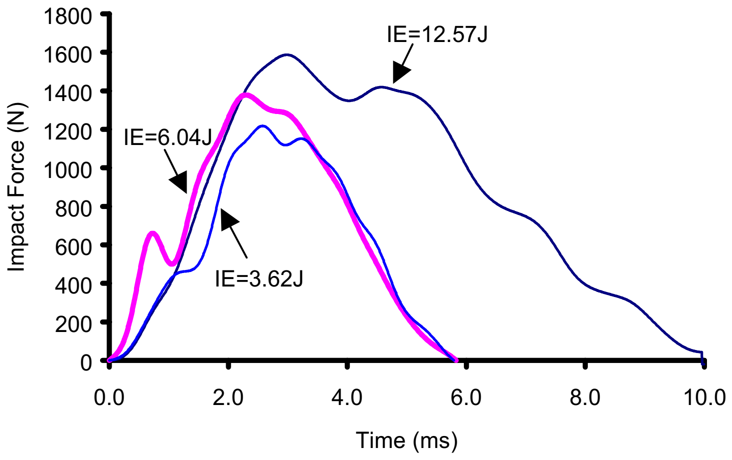

Figure 7 Representative impact force curves for $[0/0]_s$ lay-up specimens

possesses greater energy absorption ratio due to severe damage sustained under the same incident impact energy. It is also observed that crossed lay-ups possess larger structural stiffness with smaller displacement but smaller AE-ratio than that of unidirectional stacking sequences. For instance, in Fig. 8, the energy absorption ratio of 1-ply is close to 100%. As seen from Figs. 9 to 13, 2-ply specimens possess higher AE-ratio than that of 4-ply specimens. Under same incident impact energy, [0/0] specimens deflect greater than that of [0/90] specimens. For 4-ply specimens, displacements decrease in the order from $[0/0]_s$ to $[0/45]_s$ to $[0/90]_s$ specimens. It is worth to note that there exists a maximum limit of energy absorption for specimens, when incident impact energy is larger than a certain value (about 0.96J for 1-ply specimens, 3.62J for [0/90] specimens, and 6.03J for $[0/0]_s$ specimens), energy absorption ratio starts to decrease, while energy absorbed only increases slightly.

CONCLUSIONS

The IFWI test method is used to study low velocity impact damage of knitted carbon fibre/epoxy composite. C-scan and stereomicroscopy techniques are applied to examine the various damage modes and mechanisms. The study shows that unlike conventional composites, knitted composite possesses a damage mode that comes in the form of crossed-cracks, fibre/matrix debonding along path of cracks, severe fibre breakage and through-thickness cracks. This composite shows a good energy absorption capability with the energy absorption ratio capable of exceeding 80%.

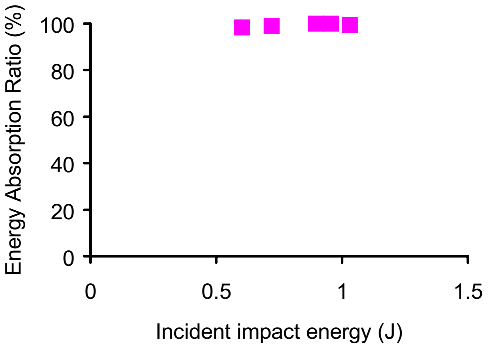

Figure 7 Impact on 1-ply specimens

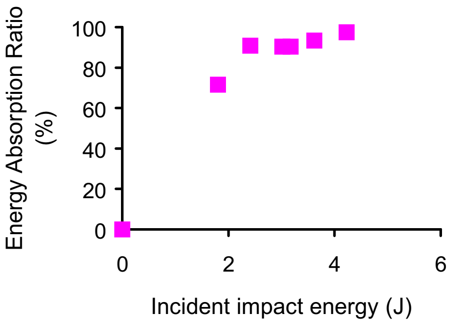

Figure 8 Impact on [0/0] specimens

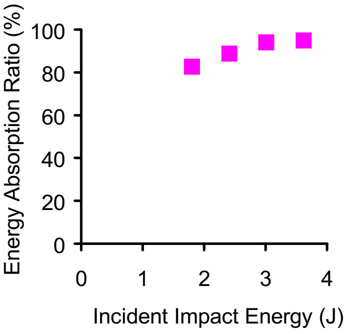

Figure 9 Impact on [0/90] specimens

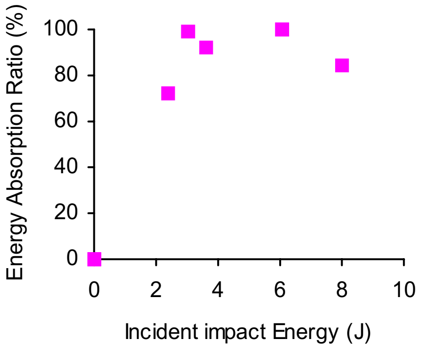

Figure 10 Impact on $[0/0]_s$ specimens

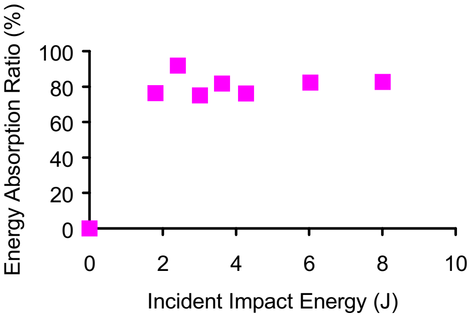

Figure 11 Impact on $[0/90]_s$ specimens

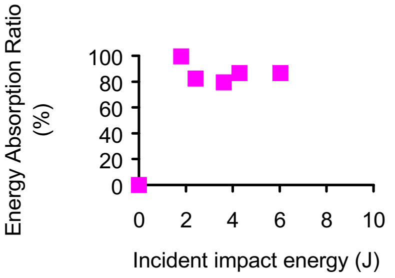

Figure 12 Impact on $[0/45]_s$ specimens

REFERENCES

[1] Robert M. Jones. *Mechanics of Composite Materials*. 2nd Edition, Taylor & Francis, 1999.
[2] Antonio Miravete (Editor). *3-D Textile Reinforcements In Composite Materials*. LRC Press, Woodhead Publishing Limited, 1999.
[3] S. T. Peters (Editor). *Handbook of Composites.* 2nd Edition. Chapman & Hall, 1998.
[4] P. K. Mallick (Editor). *Composites Engineering Handbook*, Marcel Dekker, INC. 1997.
[5] *Engineered Materials Handbook. Vol. I. Composites*, ASM International, 1987.
[6] A.P. Mouritz, M.K. Bannister, P.J. Falzon and K.H. Leong. "Reviewof applications of advanced three-dimensional fiber textile composites". *Composites Part A*, 1999; 30A: 1445-1461.

[7] J. E. McCarty. “Design and cost viability of composites in commercial aircraft”. *Composites*, 1993; 24: 361-365.

[8] C.C. Poe, Jr., H. B. Dexter and I.S. Raju. “A review of the NASA textile composites research”. *NASA-AIAA-97-1321*.

[9] I. Verpoest, Gommers and P. Van Houtte. “The potential of knitted fabrics as a reinforcement for composites”. *11th International Conference on Composite Materials*, Gold Coast, Australia, 14-18, July, 1997: I-108-113.

[10] K. Horsting, B. Wulhorst, G. Franzke and P. Offermann. “New types of textile fabrics for fibre composites”. *SAMPE Journal*, 1993, 29: 7-12.

[11] Martin B. Dow and H. Benson Dexter. “Development of stitched, braided and woven composite structures in the ACT program and Langley Research Center (1985-1997)”. *Summary and Bibliography, NASA TP 97-206234* .

[12] C. C. Poe, Jr. “Mechamicalmethodology for textile perform composites”. *NASA CP 3326.*

[13] P. Tan, L. Tong and G. P. Steven. “Modelling for predicting the mechanical properties of textile composites-A review”. *Composites Part A*, 1997; 28A: 903-922.

[14] I. Putnoki, E. Moos and J. Karger-Kocsis. “Mechanical performance of stretched knitted fabric glass fibre reinforced poly(ethylene terephthalate) composites produced from commingled yarn”. P*lastics, Rubbers and Composites*, 1999; 28(1).

[15] H Benson Dexter and Gregory H. Hasko. “Mechanical properties and damage tolerance of multiaxial warp-knit composites”. *Composites Science and Technology*, 1996; 56: 367-380.

[16] Koji Kameo, Joop De Haan, Asami Nakai and Hiroyuki. “Open hole tensile behaviours of knitted fabric composites”. *Journal of Reinforced Plastics and Composites*, 1999; 18 (17): 1605-1616.

[17] B. Gommers, I. Verpoest and P. Van Houtte. “Analysis of knitted fabric reinforced composites: Part I. Fiber orientation distribution”. *Composites Part A, 1998;* 29A: 1579-1588.

[18] E.Greenhalgh, S.Singh, D.Hughes and D.Roberts. “Impact damage resistance and tolerance of stringer stiffened composite structures”. *Plastic Rubbers and Composites*, 1999; 28(5): 228-251.

[19] J. Karger-Kocsis and T. Czigany. “Effects of interphase on the fracture and failure behavior of knitted fabric reinforced composites produced from commingled GF/PP yarn”. *Composites Part A* 1998; 29A: 1319-1330.

[20] K.H. Leong, S. Ramakrishna, Z. M. Huang and G. A. Bibo. “The potential of knitting for engineering composites - A review”, *Composites Part A, 2000;* 31A: 197-220.

[21] S. Ramakrishna and D. Hull. “Tensile Behaviour of knitted carbon-fiber-fabric/epoxy laminates-Part I: Experimental”. *Composites Science and Technology, 1994;* 50: 237-247 .

[22] S. Ramakrishna and Hamada, R.W. Rydin and T.W. Chou. “Impact damage resistance of knitted glass fiber fabric reinforced polypropylene composites”. *Science and Engineering of Composite Materials,* 1995; 14 (2): 61-72.

[23] S. Ramakrishna. “Characterization and modelling of the tensile properties of plain weft-knit fabric reinforced composites”. *Composites Science and Technology*, 1997; 57: 1-22.

[24] S. Ramakrishna. “Microstructural design of composite materials for crashworthy structural application”. *Materials and Design*, 1997; 18: 167-173.

[25] S. Ramakrishna. “Energy absorption characteristics of knitted fabric reinforced epoxy composite tubes”. *Journal of Reinforced Plastics and Composites*, 1995; 14: 1122-1141.

[26] Xiaoping Ruan and Tsu-wei Chou. “Experimental and theoretical studies of the elastic behaviour of knitted-fabric composites”. *Composites Science and Technology*, 1997; 56: 1391-1403.

[27] Zheng Ming Huang, S. Ramakrishna and . “Simulation for tensile properties of milano rib knit fabric composite laminates”. *Pro. 6th Japan, International SAMPE Symposium*, Oct. 26-29, 1999: 521-524.

[28] Zheng Ming Huang, S. Ramakrishna. “Micromechanical modelling approaches for the stiffness and strength of knitted fabric composites: a review and comparative study”. *Composites Part A*, 2000; 31A: 479-501.

[29] Guang-Wu Du and Frank Ko. “Analysis of multiaxial warp-knit performs for composites reinforcement”. *Composites Science and Technology*. 1996, 56: 253-260.

[30] H. Hamada and K. Sugimoto. “Mechanical properties of knitted fabric composites”. *Journal of Reinforced Plastics and Composites*, 2000, 19; 5: 365-376.

[31] S. Ramakrishna, H. Hamada, M. kotaki, W.L. Wu, M. Inoda and Z. Maekawa. “Future of knitted fabric reinforced polymer composites”. *Proceeding of 3rd Japan International SAMPE Symposium*, Tokyo, 1993, 312-317.

[32] J.Karger-Kocsis, Q. Yuan, J.Mayer and E. Wintermantel, “Transverse impact behaviour of knitted carbon-fibre fabric-reinforced thermoplastic composite sheets”. *Journal of Thermoplastic Composite Materials,* 1997; 10: 163-173.

[33] J. Mayer, K. Ruffieux, R Tognini and E. Wintermantel. “Knitted carbon fibres, a sophisticated textile reinforcement that offers new perspectives in thermoplastic composite processing”. *Proceeding of ECCM6*, Bordeaux, 1993: 219-224.

[34] M. B. Dow, etc. “An evaluation of stitching concepts for damage tolerant composites”. *Fibre-Tex*, 1988, *NASA CP-3038*, 1989: 53-73.

[35] W. J. Cantwell and J. Morton. “The impact resistance of composite materials - review”. *Composites*, 1991; 22 (5): 347-362.

[36] M. O. W. Richardson and M. J. Wisheart. “Review of low-velocity impact properties of composite materials”. *Composites, Part A,* 1996; 27A: 1123-1131.

[37] K. N. Shivakumar, W. Elber, and W. Illg. “Prediction of low velocity impact damage in thin circular laminates”. *AIAA Journal,* 1985, 23 (2): 442-449.

[38] P. O. Sjoblom, J. T. Hartress, and T. M. Cordell. “On low velocity impact testing of composite materials”. *Journal of Composite Materials*, 1988, 22: 30-52.